Synthesis of Hollow Responsive Functional Nanocages Using a Metal–Ligand Complexation Strategy

Alexander D. Ievins, Adam O. Moughton, and Rachel K. O'Reilly*

Melville Laboratory for Polymer Synthesis, Department of Chemistry, Lensfield Road, Cambridge, CB2 1EW, U.K.

Received January 8, 2008; In Final Form February 18, 2008; Revised Manuscript Received February 14, 2008

ABSTRACT: A metal–ligand complexation strategy using ruthenium−terpyridine interactions was utilized for the facile synthesis of amphiphilic block copolymers which were self-assembled into spherical micelles and stabilized throughout their shell to afford well-defined nanoparticles. The labile metal–ligand bond at the nanoparticle core–shell interface was then readily broken to enable excavation to afford hollow completely hydrophilic nanocages which can no longer sequester hydrophobic small molecules. These nanocages also demonstrated pH responsiveness and could be further functionalized by the reintroduction of metals.

Introduction

Recently, the design and preparation of tailor-made functionalized polymeric nanostructures has been aided by advances in controlled polymerization techniques, yet there still exists a need for new routes for the facile synthesis of functional block copolymers for applications in self-assembly. The solution self-assembly of multiblock copolymers, into nanostructured materials displaying a wide range of morphologies, has attracted considerable interest over the past decade due to their nanoscale size and unique morphologies.[1–7] These nanostructured materials have found application in a wide range of areas such as in materials science and in biomedicine, and as a result, their preparation and examination of their properties has received much interest.[8–10]

Although many techniques are available for the preparation of nanoparticles, perhaps the most versatile is the self-assembly of amphiphilic block copolymers in selective solvents, using the hydrophobic effect, to afford polymer micelles,[11–15] worm-like micelles,[16–20] or vesicles.[21–25] This method can afford well-defined phase-separated spherical micelles which contain a hydrophobic central domain which is surrounded and stabilized in aqueous media by the hydrophilic shell layer. There has been significant recent interest in the covalent stabilization of the outer corona to afford robust shell cross-linked nanoparticles which are stable to changes in concentration and temperature.[26,27] From these stabilized nanoparticle scaffolds, it was demonstrated by Wooley and co-workers that nanocages can be formed by the excavation of the core, using either ozonolytic, thermal homolytic cleavage, or hydrolytic degradation chemistry.[28–31] This afforded a hydrophilic shell layer surrounding a water-filled core or a nanocage which was capable of hydrophilic guest sequestration and further functionalization by the reintroduction of hydrophobicity.[32] However, these relatively harsh chemistries which have been previously employed for the core excavation lead to partial nanocage degradation and also ill-defined or nonreactive functionality within the interior of the nanocage. These hollow nanocages were proposed to be of interest due to their unique encapsulation potential and also further functionalization through carbonyl groups located on the cage interior surface. In more recent work, Wooley and co-workers have utilized an elegant graft copolymer route by which access to hollow nanostructures was achieved using ozonylsis.[29]

* To whom correspondence should be addressed. E-mail: rko20@cam.ac.uk. Tel: 01223 336305. Fax: 01223 334866.

A number of other methods have been reported for the synthesis of hollow cagelike materials, such as layer-by-layer deposition, microemulsion polymerization, and templating techniques, but these and other reported techniques do not offer the well-defined size, robustness, and chemical reactivity of the nanoparticle excavation method.[33–42] Another significant advantage is that the nanoparticle excavation route affords completely hydrophilic hollow nanocages which are suitable for biomedical applications and also applications in aqueous media. It is proposed that the synthesis of functional hollow nanoscale polymeric materials which display function and tunable behavior represents a significant advance toward the synthesis of synthetic biological mimics.[43–46]

There has been a growing interest in the field of supramolecular chemistry for the formation of polymers and block copolymers.[47–49] One of the easiest ways to access such systems is the placement of a noncovalent binding motif at the terminus of each of the polymer chains, such as a metal–ligand interaction, a hydrogen-bonding pair or a host–guest interaction. This allows for the synthesis of reversible and dynamic block copolymers and has been utilized to afford materials with novel properties. In particular, Jiang and co-workers have utilized hydrogen bonding non covalent interaction to great effect to form non covalently connected micelles (NCCMs). They have reported many different functional groups pairs for the noncovalent interaction; however, their work to date has focused primarily on the application of single hydrogen-bonding motifs (such as carboxylic acids and pyridine interactions) for the synthesis of the block copolymers.[50–54] Using this strategy they have been able to synthesis hollow higher ordered assembles of nanosized materials which are completely hydrophilic, via a cross-linking and subsequent cavitation.[55–57] However, much of this work has focused on the utilization of relatively ill-defined and weak interactions which has somewhat limited the scope of the resultant materials due to their dispersity and also lack of functionalization.

Our interest is in the application of more directional and stronger metal–ligand interactions to form more robust block copolymers to allow access to better defined and diverse nanostructure morphologies. Following on from the elegant work of Schubert,[58–60] Fraser,[61,62] Rowan,[63] and Weck[64] in the application of metal–ligand-based interactions for this reversible binding, we have prepared nanocages which contain functional handles located selectively throughout their interior surface. Using the reversible noncovalent interaction between the two functional

10.1021/ma800047r CCC: $40.75
Published on Web 04/30/2008

groups and a metal center, amphiphilic block copolymers have been formed in selective solvents and assembled into micelles by addition of a nonsolvent for the hydrophobic block. Following shell covalent stabilization, robust nanoparticles of well-defined size and composition have been isolated that contain a readily cleavable bond between the core and shell domains. By cleaving this bond at the interface, upon addition of a competitive ligand for the metal center and removing the core by dialysis, a hollow hydrophilic nanocage is isolated which contains reactive groups within the interior shell surface.

The methodology reported herein utilizes and builds on the extensive and pioneering work of Schubert in the area of metal−terpyridine interactions and Fraser in the area of metal−bipyridine interactions for the synthesis of metallopolymers and metallointeractions.[65,66] In particular, Schubert and Gohy have reported the application of PS and polyethylene oxide (PEO) terpyridine end-functionalized polymer blocks for the synthesis of micelles.[67–71] Recently, they also reported elegant work exploring the tailoring of the micelle size compared to conventional micelle systems with the interesting conclusion that these NCCMs did not obey the conventional scaling laws observed in covalently connected micellar systems.[72]

The method reported in this work represents a significant departure from previous nanocage synthesis reports due to the potential versatility in tailoring the nanocage to present different functionality within the shell interior. In addition, this NCCM strategy which uses metal–ligand interactions allows for the generation of selectively functionalized metal nanostructures which can be tuned and modified for advanced applications. This paper highlights this versatile and facile strategy for the synthesis of robust, well-defined hydrophilic nanocages which contain reactive and available functional groups throughout their interior shell layer.

Experimental Section

Materials. AIBN was twice recrystallized from methanol and stored in the dark at 4 °C. *t*-Butyl acrylate and styrene were distilled over CaH_2 and stored at 4 °C. Dichloromethane (CH_2Cl_2) was dried by prolonged refluxing over CaH_2. 2,2,5-Trimethyl-4-phenyl-3-azahexane-3-nitroxide,[73] 2,2,5-trimethyl-3-(1-(4′-chloromethyl)phenylethoxy)-4-phenyl-3-azahexane,[73] 2,6-bis-(pyrid-2-yl)-4-pyridone,[74] and 2,2,5-trimethyl-3-{1-[4′-(4″-terpyridinyloxy)methyl]phenylethoxy}-4-phenyl-3-azahexane, **1**, were synthesized from literature reports.[75] All other reagents were purchased from Sigma-Aldrich and were used without further purification.

Instrumentation. Hydrodynamic diameters (D_h), size distributions, and zeta potential (ζ) for the micelles and nanoparticles in aqueous solutions were determined by dynamic light scattering (DLS). The DLS instrumentation consisted of a Malvern Zetasizer Nano ZS instrument operating at 25 °C with a 635-nm laser module. Measurements were made at a detection angle of 173° (backscattering) and Malvern DTS 4.00 software using cumulant analysis was utilized to analyze the data. All determinations were made in triplicate (with 12 runs recorded).

Transmission electron microscopy samples were diluted with a 1% phosphotungstic acid (PTA) stain (1:1). Copper/carbon grids were prepared by argon plasma treatment to increase the surface hydrophilicity. Micrographs were collected at magnifications varying from 42 to 130 K and calibrated using an internal graticule. Histograms of number average particle diameters (D_{av}) and standard deviations were generated from the analysis of a minimum of 150 particles from at least three different micrographs.

Nuclear magnetic resonance (^1H and ^{13}C) were performed on a Bruker AVANCE 400 or 500 MHz FT-NMR spectrometer using deuterated solvents. Extended ^1H NMR analysis was performed to determine the M_n of the polymers by integration of the backbone or side chain signals to characteristic signals for the terpyridine end group. Gel permeation chromatography (GPC) data for all the polymers was obtained in THF (Shimadzu UFLC autosampler with Polymer Laboratories gel 5 μm Mixed C column) at room temperature with linear polymethyl methacrylate (PMMA) standards at a flow rate of 1 mL/min. The modulated differential scanning calorimetry (DSC) measurements were performed with a TA Instruments, DSC 2920 and with a ramp rate of 4°/min. Infrared (IR) spectra were obtained on Perkin-Elmer Spectrum 100 ATR FT-IR spectrometer. UV/vis spectroscopy was carried out on a Cary 4000 UV/vis spectrophotometer with Cary Win UV Scan software. Magnetic susceptibilities were determined by the Evans NMR method. According to Evans' NMR method 2−3 mg of complex was dissolved in a mixture of deuterated NMR solvent (THF-d_6) and cyclohexane (95:5 v/v) in a 1.0 mL volumetric flask. A portion of this solution was transferred into a melting point capillary tube that was sealed with PFTE tape and placed into a NMR tube containing the NMR solvent/cyclohexane mixture. The chemical shift difference (Δf) for the cyclohexane protons between the inner and outer tubes at room temperature was used to calculate the magnetic susceptibility, χ_m, and the magnetic moment, μ_{eff}.[76]

Synthesis of NMP 2,2,5-Trimethyl-3-{1-[4′-(4″-terpyridinyloxy)methyl]phenylethoxy}-4-phenyl-3-azahexane Initiator, 1. Terpyridine-functionalized initiator **1** was synthesized by reaction of 2,2,5-trimethyl-3-(1-(4′-chloromethyl)phenylethoxy)-4-phenyl-3-azahexane[73] with 2,6-bis-(pyrid-2-yl)-4-pyridone[74] via a slight modification (repeated on the same scale, but the reaction mixture was stirred for 2 days and the isolated yield was 56%) of a literature procedure.[75]

Synthesis of Terpyridine Chain End-Functionalized Poly(*t*-butyl acrylate), 2. *t*-Butyl acrylate (4.62 g, 36.4 mmol), initiator **1** (0.106 g, 0.18 mmol), and free nitroxide (0.002 g, 0.009 mmol) were placed in a dry glass ampule equipped with magnetic stirrer bar, and the solution was degassed by 3× freeze–pump–thaw cycles. The sealed vessel was then held at 120 °C for 24 h. After polymerization had occurred, the ampules were cooled in liquid N_2 and the reaction mixture diluted with THF as necessary. The polymers were precipitated into a stirred solution of cold methanol/water (10:2) and allowed to stand, and then the solvent was decanted off. After being dried over $MgSO_4$, the polymers were dried at room temperature under vacuum and then the precipitation process was repeated two further times. Terpyridine end functionalized poly(*t*-butylacrylate), **2**, was isolated as a white semicrystalline powder (2.74 g, 87%): ^1H NMR (500 MHz, $CDCl_3$) δ 8.65 (m, broad, $2H_{terpy}$), 8.56 (m, broad, $2H_{terpy}$), 8.14 (m, broad, $2H_{terpy}$), 7.87 (m, broad, $2H_{terpy}$), 7.41–6.99 (m, broad, aromatic end groups and $2H_{terpy}$), 5.24 (m, broad, terpyOCH_2), 2.30–0.37 (m, broad, polymer backbone signals, *t*-butyl groups and end groups). M_n (NMR) = 17 800 Da. M_n(GPC, THF) = 17 900 Da, M_w/M_n = 1.14. IR, ν: 2976, 2932, 1722 (ester signal), 1601, 1583, 1564 (terpyridine signals), 1479, 1447, 1392, 1366, 1253, 1142, 1032, 908, 845, 751 cm^{-1}.

Synthesis of Terpyridine Chain End-Functionalized Polystyrene, 3. Styrene (3.0 g, 28.8 mmol) and **1** (0.084 g, 0.14 mmol) were placed in a dry glass ampule equipped with magnetic stirrer bar and the solution was degassed by 3× freeze–pump–thaw cycles. The sealed vessel was then held at 120 °C for 12 h. After polymerization had occurred, the ampules were cooled in liquid N_2 and the reaction mixture diluted with THF as necessary. The polymers were precipitated into a stirred solution of excess cold methanol and filtered, and this process was repeated three times; then, the samples were dried at 40 °C under vacuum. Polymer **3** was isolated as a white powder (1.53 g, 83%): ^1H NMR (500 MHz, $CDCl_3$) δ 8.71 (m, broad, $2H_{terpy}$), 8.64 (m, broad, $2H_{terpy}$), 8.13 (m, broad, $2H_{terpy}$), 7.87 (m, broad, $2H_{terpy}$), 7.24–6.20 (m, broad, Ar−H, aromatic end groups and $2H_{terpy}$), 5.25 (m, broad, terpyOCH_2), 2.27–0.48 (m, broad, polymer backbone signals and end groups). M_n (NMR) = 13 200 Da. M_n(GPC, THF) = 12 600 Da, M_w/M_n = 1.11. IR, ν: 3026, 2923, 2849, 1602, 1583, 1564 (terpyridine signals), 1492, 1452, 1357, 1181, 1155, 1068, 1028, 906, 841, 755, 691 cm^{-1}.

Deprotection of 2 to Afford Terpyridine Chain End-Terminated Poly(acrylic acid), 4. 2 (1.00 g, 0.056 mmol, 7.6 mmol of *t*-butyl acrylate residues) was added to 20 mL of anhydrous CH_2Cl_2 at 0

°C. A 20-fold molar excess (relative to *t*-butyl acrylate residues) of trifluoroacetic acid (17.31 g, 0.151 mol) was added dropwise to the stirred solution, which was then allowed to warm to room temperature. Stirring was continued for 1 day, after which air was gently blown over the solution to remove CH_2Cl_2 and excess trifluoroacetic acid, and then 10 mL of each of THF and water were added and the solution was dialyzed into distilled water (into presoaked dialysis membrane tubes with MWCO = 3500 Da) for 2 days (incorporating eight water changes). The resultant solution was then freeze-dried to afford **4** as a fluffy white solid (0.56 g, 96%): ^{1}H NMR (500 MHz, DMSO-d_6) δ 12.2 (s, broad, OH) 8.7 (m, broad, $2H_{terpy}$), 8.6 (m, broad, $2H_{terpy}$), 8.1 (m, broad, $2H_{terpy}$), 7.9 (m, broad, $2H_{terpy}$), 7.5–7.2 (m, broad, Ar−H, aromatic end groups and $2H_{terpy}$), 5.3 (m, broad, terpyOCH_2), 2.6–0.8 (m, broad, polymer backbone signals and end groups). M_n (NMR) = 10 400 Da. IR, ν: 2948 (br), 3571, 1705 (carboxylic acid signal), 1601, 1583, 1563 (terpyridine signals), 1477, 1452, 1415, 1439, 1243, 1169, 1109, 1038, 799 cm^{-1}.

Synthesis of Ru Chain End-Complexed Polystyrene, 5. 3 (0.55 g, 0.041 mmols) and ruthenium(III) trichloride hydrate (0.042 g, 0.205 mmols) were suspended in methanol (10 mL) and heated under reflux at 80 °C for 4 h. After being cooled, the mixtures were filtered and washed with methanol and diethyl ether and then dried overnight in a vacuum oven at 40 °C to afford an orange solid, **5** (0.53 g, 96%). M_n (GPC, THF) = 13 000 Da, M_w/M_n = 1.12. IR, ν: 3061, 3026, 2922, 2845, 1601, 1583, 1564 (terpyridine signals), 1493, 1452, 1361, 1182, 1155, 1069, 1028, 906, 842, 756, 696 cm^{-1}. UV/vis (THF), λ (nm): 406, ε (mol^{-1} cm^{-1}) 5700 (Ru(III) MLCT). μ_{eff} (Evan's NMR method) = 1.76 μ_B.

Synthesis of Amphiphilic Block Copolymer, PAA-Ru-PS, 6. The two polymers **4** (0.10 g, 0.005 mmol) and **5** (0.07 g, 0.005 mmol) were mixed in a 7:3 THF/EtOH solvent system (total volume 20 mL) and heated under reflux at 70 °C for 30 min. A few drops of *N*-ethylmorpholine were then added, and the temperature maintained overnight. Upon cooling, a 10-fold molar excess of NH_4PF_6 (0.01 g, 0.05 mmol) was added and the solution stirred for 1 h. The reaction mixture was then dialyzed into a 2:1 H_2O/THF solvent system (using presoaked dialysis tubing with MWCO 12–14 kDa) for 3 days. With subsequent solvent changes, the THF content was reduced, leaving just H_2O for the final 4 days. The mixture was then freeze-dried for the removal of H_2O, leaving a fluffy pink solid, **6** (0.15 g, 88%). IR, ν: 3026, 2962, 2929, 1705, 1602, 1564 (terpyridine signals), 1493, 1452, 1259, 1248, 1167, 1111, 1028, 907, 797, 757, 693 cm^{-1}. UV/vis (THF), λ (nm): 490, ε (mol^{-1} cm^{-1}) 8600 (Ru(II) MLCT). μ_{eff} (Evan's NMR method) = 0 μ_B.

Micellization of 6 to Afford, NCCM 7. The amphiphilic metallosupramolecular block copolymer **6** (0.05 g, 1.7 mmol) was dissolved in 50 mL of THF and then 50 mL of water was added at 10 mL/h via a peristaltic pump to the stirred solution. Stirring was continued overnight and the solution was then dialyzed (into presoaked tubing with MWCO = 12–14 kDa) for 3 days, incorporating eight water changes. A very pale orange-pink, aqueous solution **7** (120 mL) resulted. The final concentration of the NCCM **7** was calculated as 0.42 mg/mL. DLS: D_h = 79 ± 3 nm. Zeta potential: ζ = −37.3 ± 0.5 mV (at pH 7.2). TEM: D_{av} = 45 ± 4 nm. A portion of **7** was freeze-dried for IR analysis. IR, ν: 2964, 2926, 1704, 1602, 1547 (terpyridine signals), 1493, 1452, 1261, 1246, 1169, 1114, 1036, 803, 757, 695 cm^{-1}. UV/vis (THF), λ (nm): 490, ε (mol^{-1} cm^{-1}) 8300 (Ru(II) MLCT).

Cross-Linking (20%) of Shell Layer of Micelle 7 to Afford Nanoparticle 8. 2,2′-(Ethylenedioxy)bis-(ethylamine) (0.0016 g, 0.01 mmol, 0.1 equiv to poly(acrylic acid) residues) in 5 mL of water was added dropwise to a vigorously stirred solution of the micelle **7** (16 mg, 40 mL). After a 1 h equilibration time, 1-[3-(dimethylamino)propyl]-3-ethylcarbodiimide methiodide (0.0065 g, 0.02 mmol, 0.2 equiv) in a 5 mL water solution was then added at 10 mL/h via a peristallic pump. The solution was stirred overnight and then dialyzed for 3 days (into presoaked tubing MWCO = 12−14 kDa) to yield a very pale orange-pink, aqueous solution **8** (50 mL). The final concentration of the NCCN **8** was calculated as 0.32 mg/mL. DLS: D_h = 71 ± 2 nm. Zeta potential: ζ = −21.3 ± 0.9 mV (at pH 7.2). TEM: D_{av} = 42 ± 3 nm. A portion of **8** was freeze-dried for IR analysis. IR, ν: 2925, 1705, 1648 (amide signal), 1602, 1564 (terpyridine signals), 1546 (amide signal), 1493, 1452, 1260, 1243, 1111, 1028, 907, 795, 757, 698 cm^{-1}. UV/vis (THF), λ (nm): 492, ε (mol^{-1} cm^{-1}) 8400 (Ru(II) MLCT).

Hollowing Out of Nanoparticle 8 to Afford Nanocage 9. A 10 000-fold molar excess of the trisodium salt of *N*-(hydroxyethyl)-ethylenediaminetriacetic acid was added to an aqueous solution of nanoparticle **8** and stirred at 60 °C for 4 h. The mixture was left to cool then dialyzed (into presoaked dialysis tubing MWCO = 25 kDa for the removal of the polystyrene core) initially into a 2:1 THF/nanopure water solution for 5 days. With subsequent solvent changes, the THF content was gradually reduced until dialysis was undertaken in nanopure water for 4 days. Overall, dialysis lasted 10 days with a total of 40 solvent changes. A white, slightly cloudy solution of nanocage **9** resulted. The final concentration of the nanocage **9** was calculated as 0.31 mg/mL. DLS: D_h = 130 ± 8 nm. Zeta potential: ζ = −23.4 ± 3.3 (at pH 7.2). TEM: D_{av} = 76 ± 6 nm. A portion of **9** was freeze-dried for IR analysis. IR, ν: 2961, 1705, 1648 (amide signal), 1602, 1580, 1564 (terpyridine signals), 1546 (amide signal), 1452, 1260, 1243, 1112, 1031, 907, 794, 758 cm^{-1}. UV/vis (THF), λ (nm): no characteristic MLCT bands observed in the region 350–600 nm.

Backfilling with Ru to Afford Metal-Lined Nanocage, 10. Ruthenium(III) chloride hexahydrate (ca. 25 mg) was added to a stirred solution of the nanocage (10 mL, 0.32 mg/mL) and then heated to 45 °C overnight, after which the solution was dialyzed into nanopure water for the removal of excess metal (MWCO ca. 6–8 kDa) then filtered using a 0.45 μm Teflon filter for the removal of insoluble aggregates. A pale orange-brown solution of **10** resulted. DLS: D_h = 146 ± 5 nm. UV/vis (H_20), λ (nm): 410 (Ru(III) MLCT), ε (mol^{-1} cm^{-1}) 4900.

Backfilling with Fe to Afford Metal-Lined Nanocage, 11. Iron(III) chloride hexahydrate (ca. 25 mg) was added to a stirred solution of the nanocages (10 mL, 0.32 mg/mL) and then heated to 45 °C overnight, after which the solution was dialyzed into nanopure water for the removal of excess metal (MWCO ca. 6–8 kDa) then filtered using a 0.45 μm Teflon filter for the removal of insoluble aggregates. A pale blue-purple solution of **11** resulted. DLS: D_h = 109 ± 4 nm. UV/vis (H_20), λ (nm): 570 (Fe(II) MLCT), ε (mol^{-1} cm^{-1}) 6200.

Sequestration Studies with Nile Red and Hollow Nanocage 9 and Nanoparticle 8. Both the nanocage, **9**, and nanoparticle, **8**, solutions (5 mL) were incubated with stirring overnight at room temperature with a solution of Nile Red in acetone (0.2 mL, 10 mg/mL). Acetone was then removed from the solutions on a rotary evaporator and these solutions were then filtered using a 0.45 μm Teflon filter for the removal of insoluble aggregates. The samples were then analyzed by UV/vis analysis (450–700 nm) to determine the hydrophobic sequestration ability of the nanostructures in solution.

pH-Dependent Studies Using Hollow Nanocage 9 and Nanoparticle 8. Nanocage **9** and nanoparticle **10** were dialyzed into a range of buffered nanopure water solutions at pHs ranging from 5 to 11 for 2 days with at least six water changes. The pH of the resultant solutions was then measured using a pH meter. The nanocage and nanoparticle samples at the range of pHs were then analyzed by DLS.

Results and Discussion

For the synthesis of chain end-functionalized amphiphilic block copolymers, careful selection of polymerization chemistries is key to ensure good end group fidelity.[77–79] Schubert and co-workers have utilized elegant and efficient post polymerization functionalization strategies, as well as functionalized initiator strategies, for the synthesis of a range of end-functionalized terpyridine polymers, and it is this latter approach which we have utilized in this work.[80–82] The application of controlled radical polymerization techniques allows for the synthesis of well-defined polymers, with good end group control

Scheme 1. Synthesis of (a) Terpyridine Chain End-Functionalized Poly(*t*-butyl acrylate), 2, Followed by Deprotection to Afford Terpyridine Chain End-Functionalized Poly(Acrylic acid), 4, and (b) Terpyridine Chain End-Functionalized Polystyrene, 3, Followed by Complexation with Ru(III) to Afford 5

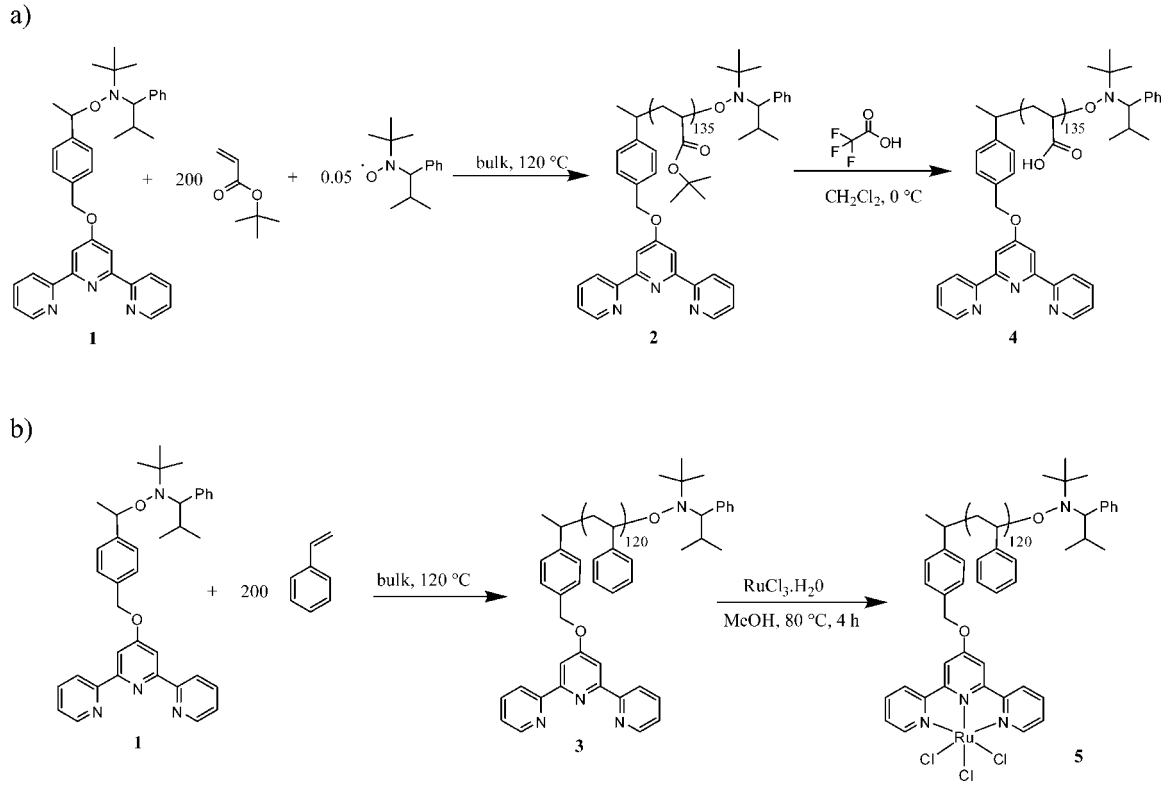

and with excellent functional group tolerance—hence, this methodology was utilized for the synthesis of the blocks.[83–88] In particular, nitroxide-mediated radical polymerization (NMP) was chosen given its controlled polymerization of a range of acrylate and styrenic monomers, as well as literature precedence for its application with terpyridine functionality in the work by Schubert and co-workers.[75] It should be mentioned that recent work by the groups of Chen and Harruna has demonstrated the application of RAFT polymerization techniques for the synthesis of end-functionalized terpyridine polymers.[89,90]

Thus, the synthesis of a terpyridine-functionalized NMP initiator, **1**, was performed as described by Schubert in 2004 and isolated in good yield.[75] This initiator was used in the polymerization of styrene and *t*-butyl acrylate (Scheme 1), to afford polymers, **2** and **3**, respectively, with well-defined molecular weights (M_n) and low polydispersities (M_w/M_n < 1.15). Blocks were targeted with degrees of polymerization (DP) around 120 and of similar block lengths to enable control of the self-assembly to afford spherical micellar morphologies (see Supporting Information for complete polymer characterization). It has been reported that the characterization of terpyridine-functionalized polymers can be problematic due to their interactions with GPC columns under standard solvent conditions.[91] However, in this work we found that the relatively small amount of terpyridine functionality incorporated into the polymer chain end did not adversely affect the obtained molecular weights by GPC analysis, and indeed, they compare very favorably to those obtained by NMR analysis (calculated by the relative integration of characteristic polymer signals and end group signals). The end group fidelity in these polymerizations was a key consideration for their application as terpyridine chain end-functionalized polymers for the synthesis of NCCMs. The presence of the terpyridine at the polymer end group was confirmed by ^{1}H NMR (characteristic terpyridine signals at ca. 8.7, 8.6, 8.1, and 7.9 ppm, all 2H) and IR (characteristic terpyridine signals at ca. 1602, 1583, and 1564 cm^{-1}) spectroscopy. In addition, the availability of this functional end group was confirmed by complexation studies of the chain end functionalized polymer **3** and a commercially available Ru(III) (Scheme 1a), as described by Schubert, followed by analysis using UV–vis spectroscopy (characteristic absorbance for a monoterpyridine Ru(III) complex at ca. 410 nm).[92,93]

To form a hydrophilic segment for utilization in the assembly of the metal–ligand-connected amphiphile the P^{t}BuA block, **2** (M_n (NMR) = 17 800, M_n (GPC) = 17 900, M_w/M_n = 1.14), was deprotected to afford a terpyridine chain end-functionalized poly(acrylic acid) (PAA) block (Scheme 1b). This was achieved using trifluoroacetic acid (TFA) under standard deprotection chemistries, which allowed for the complete removal of the ^{t}Bu groups as confirmed by IR and NMR analyses (loss of characteristic signal at 1.4 ppm in the ^{1}H NMR).[94] An important aspect of this study was the retention of terpyridine end group functionality in polymer **4** under the relatively harsh acidic ester deprotection conditions. The confirmation of the end group fidelity in **4** was achieved by ^{1}H NMR (M_n (NMR) = 10 400), IR analyses, and complexation studies followed by UV–vis spectroscopic analysis. IR analysis provided clear evidence of deprotection by the loss of ester signal at around 1722 cm^{-1} and appearance of a carboxylic acid signal at 1705 cm^{-1} with characteristic terpyridine signals still observable in the spectrum at 1601, 1583, and 1563 cm^{-1}. In addition, complexation of **4** with Ru(III) (as described for the polystyrene derivative) and UV–vis analysis confirmed the available terpyridine functionality as evidenced from the characteristic metal–ligand charge transfer bands (MLCT) bands (at ca. 405 nm) in the spectrum.

The methodology utilized for the block copolymer synthesis was performed as described by Schubert and Gohy for the synthesis of PEO-*b*-PS, terpyridine-functionalized NCCMs.[71] This involved metal complexation to the hydrophobic block followed by reaction with the hydrophilic block in a mixed

Scheme 2. Formation of the Amphiphilic Asymmetric *bis*-Terpyridine Ru(II) Polymer, 6

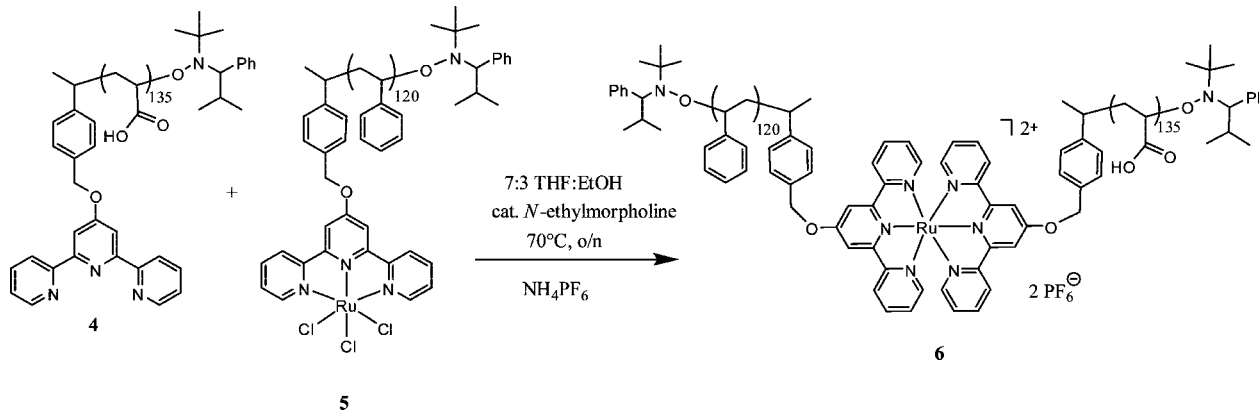

solvent system under reducing conditions. Thus initially the polystyrene block, **2** (M_n (NMR) = 13 200, M_n (GPC) = 12 600, M_w/M_n = 1.11) was complexed to $RuCl_3$ using standard literature methods to afford chain end Ru(III)-functionalized polymer **5**, which was characterized by UV/vis spectroscopy via the characteristic MLCT band at 406 nm. GPC analysis of the Ru-complexed polymer, **5**, confirmed that no polymer degradation or side reactions had occurred during the metal coupling reaction with little change in the molecular weight or polydispersity upon metal complexation (M_n (GPC) = 13 000, M_w/M_n = 1.12).

The complexation and coupling of the terpyridine chain end-functionalized **4**, PAA_{135}, and **5**, Ru-PS_{120} blocks to form a metal connected amphiphile, **6**, was performed by a modification of previously reported methods as described in Scheme 2.[71] In our experiments we utilized dialysis as a means of purification of the metal connected block copolymer. This was achieved by the careful selection of the molecular weight cutoff (MWCO = 12–14 kDa) of the tubing to ensure that upon exhaustive dialysis into a mixed THF/water system any unreacted homo blocks (M_n = 13 000 (Ru-PS) and M_n = 10 400 (PAA)) should be removed into the dialyzate. The coupling reaction appears to be very successful, as 88% yield of block copolymer was isolated after exhaustive dialysis and freeze-drying.

As reported in the literature, it was difficult to obtain GPC or definitive MALDI-ToF evidence for the block copolymer formation, due to lability of the metal–ligand bond. UV/vis and IR analysis were instead utilized to characterize the successful formation of the block copolymer, PAA_{135}(terpy)-Ru-(terpy)-PS_{120},**6**. The characteristic UV/vis MLCT band for the bis complex now appeared at 490 nm, indicating that block copolymer formation had occurred (Figure 1). In addition, the IR spectrum showed evidence of both characteristic PS (ca. 1493 cm^{-1}) and P^{t}BuA (ca. 1705 cm^{-1}) signals. Further attempts to characterize this block copolymer formation were attempted using magnetic moment analysis using Evans' NMR method. This proved to be informative as it confirmed the generation of a diamagnetic polymeric material (Ru(II)), **6**, compared to the precursor paramagnetic polymer **5** (Ru(III)), which demonstrated a μ_{eff} of 1.76 μ_B which corresponds to a Ru(III), d^5 low-spin complex.[76]

The micellar organization of these linear amphiphilic polymer chains, **6**, was performed by addition of an equal volume of water to a solution of the metal–ligand connected diblock in THF using standard solution assembly conditions. This involved **6** being dissolved in a good solvent for both blocks at 1 mg/mL, and then an equal volume of deionized water was added dropwise to this stirred solution of **6**, at a rate of ca. 10 mL/h. The resultant solution, **7**, was dialyzed against water (MWCO = 12–14 kDa) for 3 days and then analyzed by dynamic light scattering (DLS). This confirmed the presence of well-defined spherical micelles with solution hydrodynamic diameter, D_h = 79 ± 3 nm (Figure 2). In addition, the micelles were characterized by deposition onto a carbon surface, stained with phosphotungstic acid, and imaged using transmission electron microscopy (TEM); by this method, the micelle diameters were D_{av} = 45 ± 4 nm. Both these results are consistent with the formation of well-defined micelles using this metal–ligand connected micelle approach. Overall the sizes of these micelles are somewhat larger than that found for the conventionally connected diblock copolymers (for PS_{125}-*b*-PAA_{130} D_h = 65 ± 2 nm and D_{av} = 33 ± 2 nm), and this may be due to the charged counter ions from the ruthenium metal center.

To enable the hollowing out of the nanoparticle it was necessary to stabilize the hydrophilic shell layer via cross-linking chemistry. It has been reported by Wooley that the permeation of large polymeric materials through the shell layer is difficult at high cross-linking densities.[31] Given our interest in the

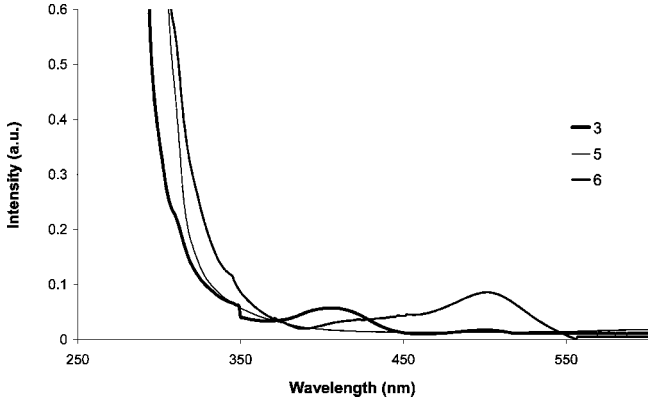

Figure 1. UV/vis spectrum in THF of homopolymer **3**, metal-complexed **5**, and amphiphilic block copolymer **6**.

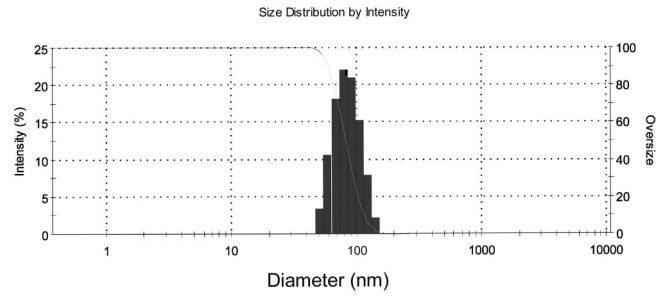

Figure 2. DLS data for the micelle, **7**, showing the size distribution and overlaid correlation function plot.

Scheme 3. (i) Assembly of Amphiphile to Form Micelle 7, (ii) Cross-Linking of Micelle 7 to Afford Nanoparticle 8, and (iii) Hollowing Out of Nanoparticle 8 to Afford Nanocage 9

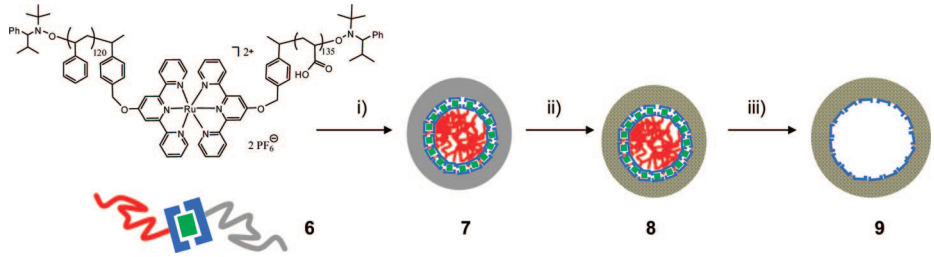

synthesis of functional nanocages, and thus the requirement for core excavation, a relatively low shell cross-linking density of 20% was targeted (**8**). This nominal degree of cross-linking was chosen for these studies, as this has been shown to impart stabilization to the nanoparticle but also maintains a high level of permeability in the shell layer.

The stabilization of these micelles was achieved by selectively cross-linking, throughout the shell layer, a fraction of the PAA groups (nominally 20%), using previously established amidation chemistries, with 2,2′-(ethylenedioxy)-*bis*(ethylamine) in the presence of 1-[3′-(dimethylamino)propyl]-3-ethylcarbodiimide methiodide.[14] The condensation reaction between the diamino cross-linkers and pendant carboxylic acid groups along the PAA segments, located in the periphery of the micelles, yielded the amphiphilic robust nanostructures. After exhaustive dialysis against water, the metal-connected nanoparticle, **8**, was isolated and characterized (Scheme 3). Zeta potential measurements (ζ) were utilized to confirm the consumption of carboxylic acid functionality in the amidation step, and the expected decrease in potential was observed from micelle **7** (−37 mV) to nanoparticle **8** (−21 mV). In addition, after freeze-drying a portion of the nanoparticle solution, IR analysis indicated the presence of amide groups (1648 and 1564 cm^{-1}) compared to the precursor micelle. The concentration of the nanoparticle solutions were determined by measurement of the final volume of nanoparticle obtained together with the initial weight of the polymer precursors used.

The size and shape of the nanoparticle **8** were measured on a solid substrate by transmission electron microscopy (TEM, Figure 3) and in solution using dynamic light scattering (DLS). Significantly, TEM analysis gave nanoparticle diameters (D_{av}) which were smaller than the respective diameters obtained from DLS analysis (D_h) (Table 1).

The hollowing out of these nanoparticles was investigated using a method similar to that recently reported by Schubert.[95] The nanoparticle, **8**, was reacted in aqueous solution at 60 °C, with a large excess of *N*-hydroxyethylethylenediamine triacetic acid sodium salt (HEEDTA), which is a competitive binder for the Ru center, for 4 h and then dialyzed into a THF/water (2:1) solution for 5 days. After this time the THF concentration of the dialyzate was slowly reduced to zero and the resultant nanostructure, **9**, was dialyzed against deionized water for a further 4 days. This resulted in a total of 40 water changes, which is a significantly higher number than reported for the nanoparticle purification and was performed due to the proposed

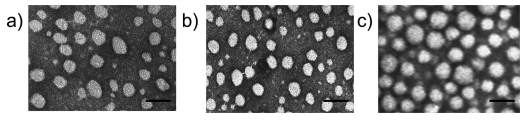

Figure 3. TEM images of (a) micelle **7**, (b) nanoparticle **8**, and (c) nanocage **9**. Scale bar shown is 100 nm. Samples were stained with phosphotungstic acid, drop deposited onto a carbon-coated copper grid and allowed to dry under ambient conditions.

increased difficulty in removing a polymer chain compared to a small molecule. After this time the nanostructures were analyzed by light scattering and were found to have significantly increased in size, D_h (of **9**) = 130 ± 8 nm. This is not surprising, as core excavation removes the constraints which the rigid polystyrene core had imparted on the nanoparticles. This has been observed previously by Wooley and provided initial evidence that indeed the excavation step had been successful.[28] In addition, after freeze-drying a portion of the nanocage solution, IR analysis indicated the absence of signals attributable to the polystyrene polymer (ca. 700 cm^{-1}).

This methodology is proposed to completely remove the metal center from the nanostructure, and this was evidenced both in a loss of pink-orange color in the solution and also by UV/vis absorbance in which no MLCT bands were now visible. However, this methodology is proposed to afford a nanocage with a terpyridine functional handle available throughout its interior shell surface and this was tenuously confirmed by freeze-drying of the sample followed by IR analysis in which the terpyridine functional groups were visible (1602, 1580, and 1564 cm^{-1}). However, further evidence was provided by the back-filling of the hollow nanocage with a second metal center to enable the reintroduction of the metal centers into the now hollow hydrophilic nanostructures. This was performed by reacting the nanocage **9** with commercially available iron and ruthenium trihalide precursors using similar conditions as reported in the literature for the complexation of terpyridine-functionalized hydrophilic block copolymers.[93,96] The novel nanocages were then purified by exhaustive dialysis and also through a Teflon filter (0.45 μm) to remove aggregates to afford a pale orange-brown solution of **10** for the ruthenium derivative and a pale purple solution of **11** for the iron analogue. These two nanocages were analyzed by DLS, a size increase of around 16 nm was observed for the ruthenium analogue, and a size decrease of 21 nm was observed for the iron analogue compared to the precursor nanocage, **9**, which did not contain metal centers. It is proposed given the literature precedence that the ruthenium analogue forms a mono-complexed metal center, but the iron derivative forms a bis complex, which can be envisaged as causing the cross-linking or collapse of the nanocage. In addition, the two nanocage solutions were analyzed by UV/vis spectroscopic analysis and showed characteristic absorbances for either mono-complexed terpyridine MLCT for **10** (ca. 410 nm) and suggested possible bis-complexed terpyridine MLCT for **11** (ca. 570 nm).[81,95]

To confirm the hollow nature of the nanostructures, and thus complete removal of the hydrophobic core domain, sequestration studies were performed using a hydrophobic dye molecule. Nile Red was chosen given its absorbance in a region (ca. 550 nm) of the spectrum which is far removed from the absorbances due to the polymer or nanostructure (around and below 300 nm). Sequestration studies using Nile Red were utilized to confirm if an entirely hydrophilic hollow nanocage had been synthesized due to the different sequestration ability of the proposed cage,

Table 1. Characterization Data for Micelle 7 and the Corresponding Nanoparticle 8 and Nanocage 9

particle	DLS D_h[a] (nm)	TEM D_{av}[b] (nm)	ζ[c](mV)
7	79 ± 3	45 ± 4	-37 ± 1
8	71 ± 2	42 ± 3	-21 ± 1
9	130 ± 8	76 ± 6	-23 ± 3

[a] Number-averaged hydrodynamic diameters in aqueous solution by DLS. [b] Average diameters were measured by TEM, calculated from the values for 150 particles. [c] Zeta potential, from 12 determinations of five runs.

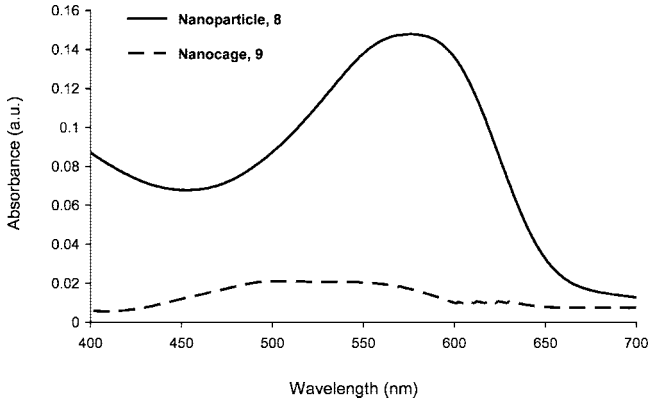

Figure 4. UV/vis data for the sequestration studies using Red Nile dye and nanoparticle **8** and nanocage **9**.

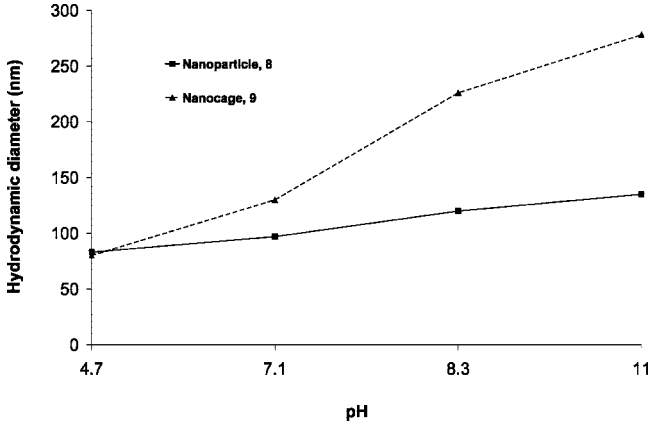

Figure 5. pH-dependent DLS measurements for nanoparticle **8** and nanocage **9**.

9, compared to the parent nanoparticle, **8**. This was achieved using previously reported techniques and is described in the Supporting Information.[32,97] Analysis of the resultant solutions by UV/vis spectroscopy confirmed the formation of a hydrophilic structure which is incapable of sequestering small hydrophobic molecules compared to its precursor nanoparticle, **8** (Figure 4). This provides further convincing evidence for the hollow and completely hydrophilic nature of the resultant nanostructure.

Our interest in these hollow materials is due to their encapsulation and release potential for applications in drug, gene, or small-molecule delivery.[98–101] These applications are proposed to be facilitated by the ability for the PAA acid shell to swell and contract because of the electrostatic interactions throughout the layer. Hence, we proposed that the nanocage structure, **9**, may be able to demonstrate pH-sensitive size dependence in analogy to naturally occurring viruses.[102] Thus, using DLS measurements, the size and pH relationship were investigated for the nanocage **9** and compared to the parent nanoparticle **8** (Figure 5). As expected, the nanocage demonstrated a pH-dependent size which was significantly more pronounced than for the parent nanoparticle. This can be attributed to the removal of the glassy polystyrene core domain which enables the nanoparticle to swell and contract more readily. This pH-dependent size was found to be reversible, and the size of nanocage **9** could be readily cycled between ca. 90 and 240 nm by changing the pH between 5 and 9. However, at pH's outside this range, some precipitation of the nanocage was observed.

Conclusion

This work introduces a versatile strategy for the synthesis of functional hollow nanoparticles using the extensive and well-established chemistry for the chain end-functionalization of block copolymers via controlled radical polymerization techniques. In conjunction with noncovalent bonding pairs, amphiphilic block copolymers have been isolated and assembled into spherical micellar morphologies, stabilized, and then selectively excavated using mild chemistries. By simultaneously utilizing reactive terpyridine groups as part of the noncovalent bonding pair, functional groups for metal complexation have been selectively introduced at the core–shell interface of the nanoparticle. The further functionalization of the nanocages, and thus application as delivery vessels via backfilling with hydrophobic moieties or other metals, is currently under investigation and will be reported elsewhere.

Acknowledgement. The authors thank the IRC in Nanotechnology, EPSRC, the Royal Society, Nuffield Foundation, and Downing College for funding.

Supporting Information Available: Select further characterization. This material is available free of charge via the Internet at http://pubs.acs.org.

References and Notes

(1) Zhang, L. F.; Yu, K.; Eisenberg, A. *Science* **1996**, *272*, 1777–1779.
(2) Zhang, L. F.; Eisenberg, A. *J. Am. Chem. Soc.* **1996**, *118*, 3168–3181.
(3) Webber, S. E. *J. Phys. Chem. B* **1998**, *102*, 2618–2626.
(4) Discher, D. E.; Eisenberg, A. *Science* **2002**, *297*, 967–973.
(5) Matejicek, P.; et al. *Macromolecules* **2002**, *35*, 9487–9496.
(6) Chen, Z.; et al. *J. Am. Chem. Soc.* **2005**, *127*, 8592–8593.
(7) Butun, V.; Lowe, A. B.; Billingham, N. C.; Armes, S. P. *J. Am. Chem. Soc.* **1999**, *121*, 4288–4289.
(8) Wooley, K. L. J. *Polym. Sci., Part A: Polym. Chem.* **2000**, *38*, 1397–1407.
(9) Lodge, T. P. *Macromol. Chem. Phys.* **2003**, *204*, 265–273.
(10) Ma, Q.; Remsen, E. E.; Kowalewski, T.; Wooley, K. L. *J. Am. Chem. Soc.* **2001**, *123*, 4627–4628.
(11) Ding, J. F.; Liu, G. J. *Macromolecules* **1998**, *31*, 6554–6558.
(12) Wooley, K. L. *Chem.−Eur. J.* **1997**, *3*, 1397–1399.
(13) Thurmond, K. B.; Kowalewski, T.; Wooley, K. L. *J. Am. Chem. Soc.* **1996**, *118*, 7239–7240.
(14) Thurmond, K. B.; Kowalewski, T.; Wooley, K. L. *J. Am. Chem. Soc.* **1997**, *119*, 6656–6665.
(15) Cao, L.; Manners, I.; Winnik, M. A. *Macromolecules* **2001**, *34*, 3353–3360.
(16) Won, Y.-Y.; Paso, K.; Davis, H. T.; Bates, F. S. *J. Phys. Chem. B* **2001**, *105*, 8302–8311.
(17) Massey, J.; Power, K. N.; Manners, I.; Winnik, M. A. *J. Am. Chem. Soc.* **1998**, *120*, 9533–9540.
(18) Kim, Y.; Dalhaimer, P.; Christian, D. A.; Discher, D. E. *Nanotechnology* **2005**, *16*, S484–S491.
(19) Li, Y.; Liu, G. *Langmuir* **2003**, *19*, 10480–10486.
(20) Yoshida, T.; Taribagil, R.; Hillmyer, M. A.; Lodge, T. P. *Macromolecules* **2007**, *40*, 1615–1623.
(21) Choucair, A.; Lavigueur, C.; Eisenberg, A. *Langmuir* **2004**, *20*, 3894–3900.
(22) Terreau, O.; Luo, L. B.; Eisenberg, A. *Langmuir* **2003**, *19*, 5601–5607.
(23) Discher, B. M.; et al. *Science* **1999**, *284*, 1143–1146.
(24) Zhang, L. F.; Eisenberg, A. *Science* **1995**, *268*, 1728–1731.
(25) Nardin, C.; Hirt, T.; Leukel, J.; Meier, W. *Langmuir* **2000**, *16*, 1035–1041.

(26) O'Reilly, R. K.; Hawker, C. J.; Wooley, K. L. *Chem. Soc. Rev* **2006**, *35*, 1068–1083.
(27) Read, E. S.; Armes, S. P. *Chem. Commun.* **2007**, 3021–3035.
(28) Huang, H. Y.; Remsen, E. E.; Kowalewski, T.; Wooley, K. L. *J. Am. Chem. Soc.* **1999**, *121*, 3805–3806.
(29) Cheng, C.; Qi, K.; Khoshdel, E.; Wooley, K. L. *J. Am. Chem. Soc.* **2006**, 6808–6809.
(30) Ma, Q.; et al. *Nano. Lett.* **2001**, *1*, 651–655.
(31) Murthy, K. S.; et al. *Chem. Commun.* **2001**, 773–774.
(32) Turner, J. L.; Chen, Z.; Wooley, K. L. *J. Controlled Release* **2005**, *109*, 189–202.
(33) Katagiri, K.; Matsuda, A.; Caruso, F. *Macromolecules* **2006**, *39*, 8067–8074.
(34) Jang, J.; Lee, K. *Chem. Commun.* **2002**, 1098–1099.
(35) Wang, J.; Jiang, M. *J. Am. Chem. Soc.* **2006**, *128*, 3703–3708.
(36) Zhang, Y.; et al. *Adv. Funct. Mater.* **2005**, *15*, 695–699.
(37) Donath, E.; et al. *Angew. Chem., Int. Ed.* **1998**, *37*, 2201–2205.
(38) Wendland, M.; Zimmerman, S. C. *J. Am. Chem. Soc.* **1999**, *121*, 1389–1390.
(39) Kim, D.; et al. *Angew. Chem., Int. Ed.* **2007**, *46*, 3471–3474.
(40) Sauer, M.; Meier, W. *Chem. Commun.* **2001**, 55–56.
(41) Han, J.; Song, G.; Guo, R. *Adv. Mater.* **2006**, *18*, 3140–3144.
(42) Sanji, T.; Nakatsuka, Y.; Ohnishi, S.; Sakurai, H. *Macromolecules* **2000**, *33*, 8524–8526.
(43) Meier, W. *Chem. Soc. Rev.* **2000**, *29*, 295–303.
(44) Hamley, I. M. *Soft Matter* **2005**, *1*, 36–43.
(45) Chen, D. Y.; Jiang, M. *Acc. Chem. Res.* **2005**, *38*, 494–502.
(46) Peyratout, C. S.; Dahne, L. *Angew. Chem., Int. Ed.* **2004**, *43*, 3762–3783.
(47) Brunseld, L.; Folmer, B. J. B.; Sijbesma, R. P.; Meijer, E. W. *Chem. Rev.* **2001**, *101*, 4071–4097.
(48) Elemans, J. A. A. W.; Rowan, A. E.; Nolte, R. J. M. J. *Mater. Chem.* **2003**, *13*, 2661–2670.
(49) South, C. R.; Budd, C.; Weck, M. *Acc. Chem. Res.* **2007**, *40*, 63–74.
(50) Zhang, Y.; Xiang, M.; Jiang, M.; Wu, C. *Macromolecules* **1997**, *30*, 6084–6089.
(51) Kawakami, T.; Kato, T. *Macromolecules* **1998**, *31*, 4475–4479.
(52) Wang, M.; et al. *Macromolecules* **2001**, *34*, 7172–7178.
(53) Yuan, X. F.; et al. *Langmuir* **2001**, *17*, 6122–6126.
(54) Ciferri, A. *Macromol. Rapid Commun.* **2002**, *23*, 511–529.
(55) Zhang, Y.; et al. *Macromolecules* **2004**, *37*, 1537–1543.
(56) Duan, H.; et al. *J. Am. Chem. Soc.* **2001**, *123*, 12097–098.
(57) Wang, M.; et al. *Macromolecules* **2002**, *35*, 5980–5989.
(58) Lohmeijer, B. G. G.; Schubert, U. S. *J. Polym. Sci., Part A: Polym. Chem.* **2003**, *41*, 1413–1427.
(59) Hofmeier, H.; Schubert, U. S. *Chem. Soc. Rev.* **2004**, *33*, 373–399.
(60) Andres, P. R.; Schubert, U. S. *Adv. Mater.* **2004**, *16*, 1043–1068.
(61) Fraser, C. L.; Smith, A. P.; Wu, X. *J. Am. Chem. Soc.* **2000**, *122*, 9026–9027.
(62) Lamba, J. J. S.; Fraser, C. L. *J. Am. Chem. Soc.* **1997**, *119*, 1801–1802.
(63) Beck, J. B.; Ineman, J. M.; Rowan, S. J. *Macromolecules* **2005**, *38*, 5060–5068.
(64) Pollino, J. M.; Weck, M. *Chem. Soc. Rev.* **2005**, *34*, 193–207.
(65) Hofmeier, H.; et al. *Aust. J. Chem.* **2004**, *57*, 419–426.
(66) Smith, A. P.; Fraser, C. L. *Macromolecules* **2003**, *36*, 2654–2660.
(67) Gohy, J. F.; Lohmeijer, B. G. G.; Schubert, U. S. *Macromol. Rapid Commun.* **2002**, *23*, 555–560.
(68) Gohy, J. F.; et al. *Macromolecules* **2002**, *35*, 9748–9755.
(69) Gohy, J. F.; Lohmeijer, B. G. G.; Varshney, S. K.; Schubert, U. S. *Macromolecules* **2002**, *35*, 7427–7435.
(70) Gohy, J. F.; Hofmeier, H.; Alexeev, A.; Schubert, U. S. *Macromol. Chem. Phys.* **2003**, *204*, 1524–1530.
(71) Gohy, J. F.; Lohmeijer, B. G. G.; Schubert, U. S. *Macromolecules* **2002**, *35*, 4560–4563.
(72) Guillet, P.; et al. *Macromolecules* **2006**, *39*, 5484–5488.
(73) Benoit, D.; Chaplinski, V.; Braslau, R.; Hawker, C. J. *J. Am. Chem. Soc.* **1999**, *121*, 3904–3920.
(74) Schubert, U. S.; Schmatloch, S.; Precup, A. A. *Des. Monom. Polym.* **2002**, *5*, 211–221.
(75) Lohmeijer, B. G. G.; Schubert, U. S. *J. Polym. Sci., Part A: Polym. Chem.* **2004**, *42*, 4016–4027.
(76) Evans, D. F. *J. Chem. Soc.* **1959**, 2003–2006.
(77) Hoogenboom, R.; Schubert, U. S. *Chem. Soc. Rev.* **2006**, *35*, 622–629.
(78) Smith, A. P.; Fraser, C. L. *Macromolecules* **2002**, *35*, 594–596.
(79) Smith, A. P.; Fraser, C. L. *Macromolecules* **2003**, *36*, 5520–5525.
(80) Lohmeijer, B. G. G.; Schubert, U. S. *Macromol. Chem. Phys.* **2003**, *204*, 1072–1078.
(81) Lohmeijer, B. G. G.; Schlaad, H.; Schubert, U. S. *Macromol. Symp.* **2003**, *196*, 125–135.
(82) Lohmeijer, B. G. G.; Schubert, U. S. *Angew. Chem., Int. Ed.* **2002**, *41*, 3825–3829.
(83) Hawker, C. J.; Bosman, A. W.; Harth, E. *Chem. Rev.* **2001**, *101*, 3661–3688.
(84) Matyjaszewski, K.; Xia, J. H. *Chem. Rev.* **2001**, *101*, 2921–2990.
(85) Kamigaito, M.; Ando, T.; Sawamoto, M. *Chem. Rev.* **2001**, *101*, 3689–3745.
(86) Chiefari, J.; et al. *Macromolecules* **1998**, *31*, 5559–5562.
(87) Georges, M. K.; Veregin, R. P. N.; Kazmaier, P. M.; Hamer, G. K. *Macromolecules* **1993**, *26*, 2987–2988.
(88) Mayadunne, R. T. A.; et al. *Macromolecules* **1999**, *32*, 6977–6980.
(89) Zhang, L.; Zhang, Y.; Chen, Y. *Eur. Polym. J.* **2006**, *42*, 2398–2406.
(90) Zhou, G.; Harruna, I. I. *Macromolecules* **2005**, *38*, 4114–4123.
(91) Meier, M. A. R.; Lohmeijer, B. G. G.; Schubert, U. S. *Macromol. Rapid Commun.* **2003**, *24*, 852–857.
(92) Schubert, U. S.; Hofmeier, H. *Macromol. Rapid Commun.* **2002**, *23*, 561–566.
(93) Heller, M.; Schubert, U. S. *Macromol. Rapid Commun.* **2002**, *23*, 411–415.
(94) Ma, Q.; Wooley, K. L. *J. Polym. Sci., Part A: Polym. Chem.* **2000**, *38*, 4805–4820.
(95) Hofmeier, H.; Schubert, U. S. *Macromol. Chem. Phys.* **2003**, *204*, 1391–1397.
(96) Chiper, M.; Meier, M. A. R.; Kranenburg, J. M.; Schubert, U. S. *Macromol. Chem. Phys.* **2007**, *208*, 679–689.
(97) Turner, J. L.; Wooley, K. L. *Nano Lett.* **2004**, *4*, 683–688.
(98) Dou, H.; et al. *Angew. Chem., Int. Ed.* **2003**, *42*, 1516–1519.
(99) Rodriguez-Hernandez, J.; Lecommandoux, S. *J. Am. Chem. Soc.* **2005**, *127*, 2026–2027.
(100) Du, J.; Tang, Y.; Lewis, A. L.; Armes, S. P. *J. Am. Chem. Soc.* **2005**, *127*, 17982–17983.
(101) Morishima, Y. *Angew. Chem., Int. Ed.* **2007**, *46*, 1370–1372.
(102) Liepold, L. O.; et al. *Phys. Biol.* **2005**, *2*, S166–S172.

MA800047R